SOLFEO

ESA Contract No 4000127610/19/I-NS

User manual
NOx emissions

Date of issue: 13 August 2020

Author(s): Ronald van der A

Table of Contents

1 Introduction

1.1 Service description

Up-to-date and reliable emission inventories are essential for accurate air quality modelling and forecasting on various spatial scales. These inventories are also used by policy makers to evaluate the effectiveness of emission abatement measures, and to decide on future strategies. Unfortunately, traditional bottom-up emission inventories are often inaccurate and are always a few years behind the actual developments. Inventory updates (if available at all) are usually based on partly updates of the underlying proxy data, leading to different time frames for different sectors and sources. Satellite observations of air constituents provide an alternative way of estimating emissions. The main advantage of these top-down emission estimates are the spatial and temporal consistency for all sectors and pollutants, a high temporal resolution, and the rapid availability.
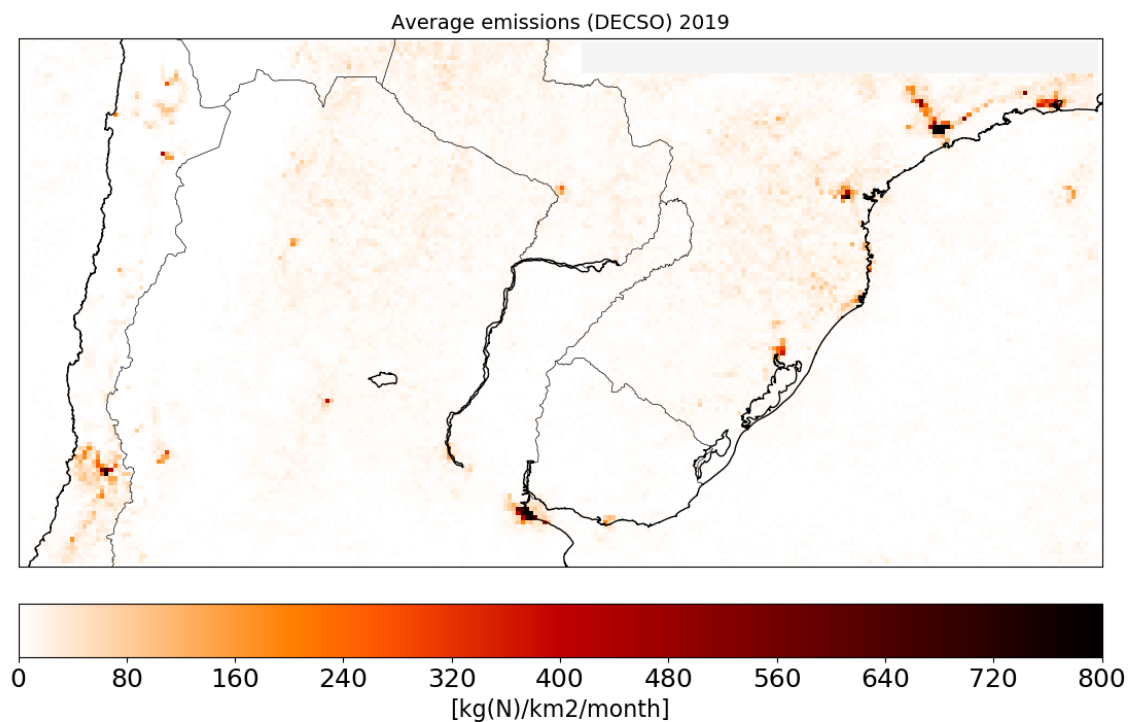
Figure 1. NO_x emission for the year 2019 derived from the TROPOMI satellite using the DECSO algorithm.

1.2 DECSO algorithm description

The DECSO algorithm [Mijling and Van der A, 2012] is specifically designed to use daily satellite observations of column concentrations for fast updates of emission estimates of short-lived atmospheric constituents on a mesoscopic scale (0.25°×0.25°). An extensive description of the algorithm can be found in the GlobEmission ATBD [2015].

We use the DECSO algorithm together with the regional CTM CHIMERE [Schmidt et al, 2001; Bessagnet et al., 2004] on a 0.25° resolution, driven by operational meteorological forecast of the European Centre for Medium-Range Weather Forecasts (ECWMF). The CTM implementation is described in more detail by Mijling et al. [2009]. We use NO_2 observations from the OMI or the GOME-2 instrument. From 1 January 2013 onward, the DECSO-v3a series for GOME-2 are based on GOME-2B retrievals. Tropospheric NO_2 column retrievals are calculated with the DOMINO v2 algorithm [Boersma et al., 2011] from spectral measurements between 426–451 nm. This data is available through the TEMIS portal (http://www.temis.nl). Cloud fraction and cloud height are derived from the oxygen-A band [Koelemeijer et al., 2001]. NO_2 retrievals at cloud fractions larger than 20% are filtered out to reduce the influence of the modelled NO_2 column below the clouds. Retrievals with low clouds (below 800 hPa) are also rejected because the intersection of the cloud with the NO_x bulk makes the retrieval too sensitive for the exact cloud height. Before comparing the model simulations with the satellite observations, the CHIMERE vertical profiles are extended from the model ceiling (at 500 hPa) to the tropopause with a climatological partial column. The profiles are then interpolated to the observational footprints (having a lower spatial resolution), after which the averaging kernel can be directly applied, see Mijling and Van der A [2012].
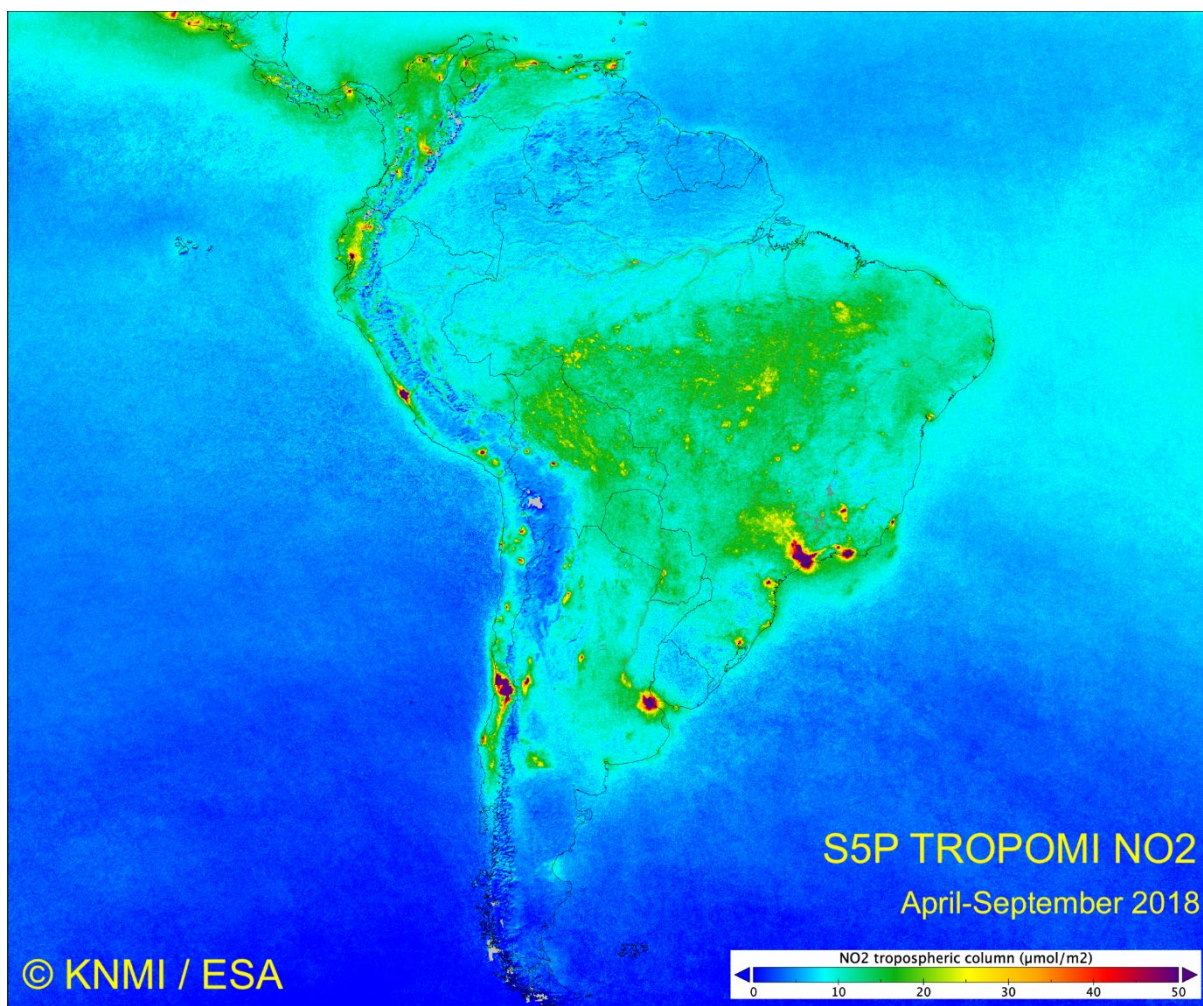
Figure 2   Averaged tropospheric NO2 columns as observed by the S5 TROPOMI instrument in the summer of 2018.

2 Product Specifications

2.1 Product description

Table 1. Output product description for emission inventory.

Product Type	Emission inventory. Air pollutants included: NO_x (NO_2+NO)
Spatial Resolution	0.125 degrees
Temporal Range	July 2018 – December 2019
Temporal Resolution	Monthly averaged
Estimated accuracy	20%
Spatial Coverage	Domain 1: 36-22° S, 60-42° W Domain 2: 36-21° S, 73-57° E
Format and Size	Format: netCDF Size: approximately 1.6 MB per file
Satellite data sources	TROPOMI

- The NOx (nitrogen oxide) emissions based on TROPOMI for South America can be found at http://www.globemission.eu/region_samerica/datapage_nox.php

2.2 Data structure

In tables 15-20 the foreseen data structures of the GlobEmission emission inventories are presented. In principle, the meta data description as well as the variables describe the data set in it full extend. The meta data have been harmonised among the partners and include the data origin, comments, and all emission category and domain descriptors. As such the foreseen data products will be compliant with GEOSS recommendations ensuring easy access to the data.

Table.2 Data structure for regional DECSO emission data in South America.

Attribute	Meta Data Description
X1: Description	Product desciption
X2: Author	name of creator
X3: Institution	name of institute
X4: Domain	Region with available data
X5: Year	Time period of emission inventory
X6: History	Date of creation
X7: grid_west	west bound of regular grid
X8: grid_west_unit	units of west bound of regular grid
X9: grid_east	east bound of regular grid
X10: grid_east_unit	units of east bound of regular grid
X11: grid_lon_res	longitudinal resolution of regular grid
X12: grid_lon_res_unit	units of longitudinal resolution of regular grid
X13: grid_south	south bound of regular grid
X14: grid_south_unit	units of south bound of regular grid
X15: grid_north	north bound of regular grid
X16: grid_north_unit	units of north bound of regular grid
X17: grid_lat_res	latitudinal resolution of regular grid
X18: grid_lat_res_unit	units of latitudinal resolution of regular grid
Variable	**Description + unit**
V1: time	Time in days since the beginning of the year
V2: lat	cell latitudes in regular grid (cell centers) [degrees_north]
V3: lon	cell longitudes in regular grid (cell centers) [degrees_east]
V4: NOx	nitrogen-oxides emission from source [10^{15} molecules/cm2/h]
V5: NOx_alt	nitrogen-oxides emission from source [Gg N/cell/month]
V6: area	cell area in regular grid [km2]
Dimensions	**Definition**
time	Dimension of the time variable
lat	Dimension of the variable lat
lon	Dimension of the variable lon

3 Data quality

3.1 High altitudes

The CTM used in DECSO is modeling till a pressure level of about 500 hPa. For very high mountain ranges this can lead to too small model layers with unrealistic local model results. This can lead to unrealistic emissions over the Andes. Therefore, all data for grid cells with an average altitude above 3500 m has been removed. Figure 2 shows the altitude in the region of the emissions.
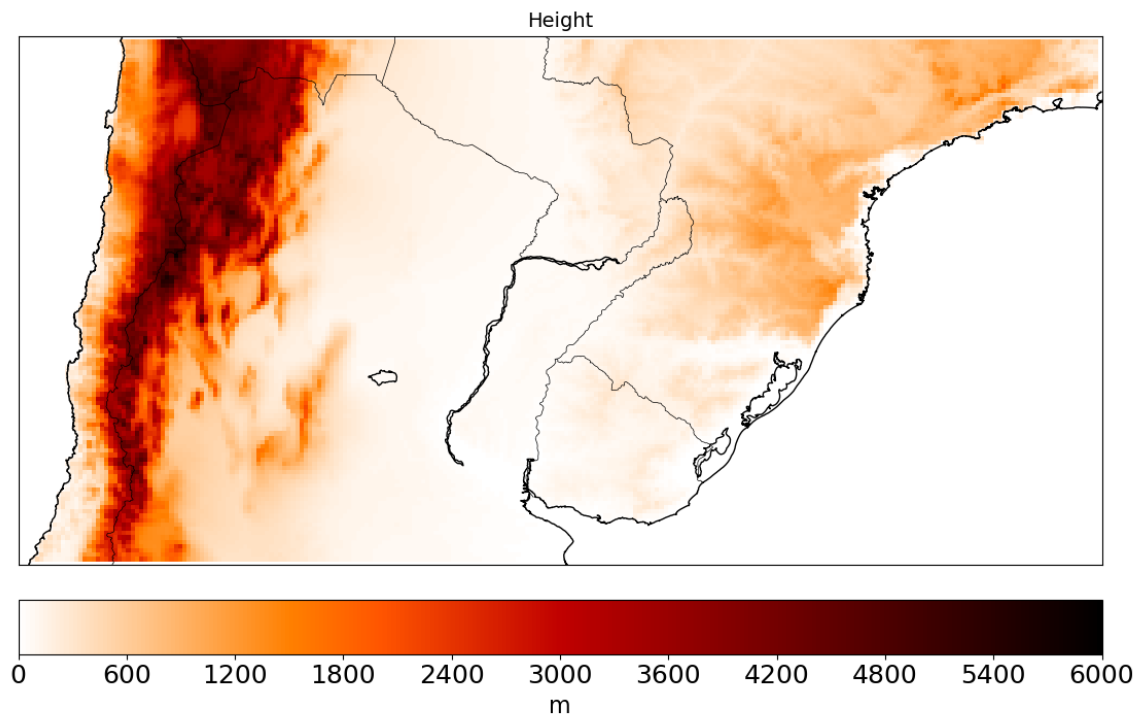
Figure 3 Surface altitude in the region for which the emissions are provided.

3.2 TROPOMI NO2 validation

The validation activities for TROPOMI versions 1.2 and 1.3 have clearly indicated that the tropospheric NO2 column product is low compared to independent observations, in particular against MAX-DOAS, PANDORA and aircraft campaign data. Typically, for the MAX-DOAS instruments a bias of -30% is reported in the routine validation activity (the Mission Performance Centre) for TROPOMI.

Two main observations are of relevance for the emissions:

- Comparisons against MAXDOAS indicate that the bias is multiplicative, increasing linearly with the column amount. The slant column observations and stratospheric column agree well with SAOZ and PANDORA. The linearity indicates that mainly the air-mass factor is involved.
- An analysis of the retrieval attributes the low bias to three main effects: (1) a bias in the cloud pressure retrieval which substantially impacts the low cloud fraction retrievals; (2) a high bias in the albedo, and (3) the coarse resolution of the a-priori profiles (1x1 degree). We estimate

that roughly half of the systematic low bias at NO_2 hotspots is related to the a-priori profile shape (point 3). However, this part of the bias does not influence the results presented in our study. The reason is that we explicitly make use of the TROPOMI averaging kernels, which makes the emission results independent of the retrieval a-priori profile shape.

In conclusion, a typical systematic absolute bias of about 15% will remain, and we expect the emissions to be low by such an amount on average.

Related validation papers:

Judd, L. M., Al-Saadi, J. A., Szykman, J. J., Valin, L. C., Janz, S. J., Kowalewski, M. G., et al. (2020). Evaluating Sentinel-5P TROPOMI tropospheric NO2 column densities with airborne and Pandora spectrometers near New York City and Long Island Sound. Atmos. Meas. Tech. Discuss., 2020, 1-52. doi:10.5194/amt-2020-151

Tack, F., Merlaud, A., Iordache, M. D., Pinardi, G., Dimitropoulou, E., Eskes, H., et al. (2020). Assessment of the TROPOMI tropospheric NO2 product based on airborne APEX observations. Atmos. Meas. Tech. Discuss., 2020, 1-55. doi:10.5194/amt-2020-148

Verhoelst, T., Compernolle, S., Pinardi, G., Lambert, J. C., Eskes, H. J., Eichmann, K. U., et al. (2020). Ground-based validation of the Copernicus Sentinel-5p TROPOMI NO2 measurements with the NDACC ZSL-DOAS, MAX-DOAS and Pandonia global networks. Atmos. Meas. Tech. Discuss., 2020, 1-40. doi:10.5194/amt-2020-119

3.3 Validation of version 5.0 over China

NOx estimates are done with our in-house developed, state-of the-art DECSO algorithm. Various versions of the DECSO algorithm have been validated in various papers. Validation of the latest version 5.0/5.1 is described in Ding et al. [2018], Ding et al. [2017a], and Ding et al. [2017b]. In general, the uncertainty of the monthly averaged NOx emissions is 20%. Currently, OMI observations are used for NOx emission estimates. We use the latest retrieval version (QA4ECV) for the satellite data. Higher resolution emissions became also available using TROPOMI retrievals, taking advantage of the superior spatial resolution and signal-to-noise ratio of this instrument. These higher resolution emissions of TROPOMI are only processed for smaller domains like the Iberian Peninsula.

## 3.4 Verification of version 5.2 over the Iberian peninsula

Within the CHE project DECSO v5.2 has been compared with TNO industrial 2010 NOx emissions over the Iberian Peninsula on a 1/8 degree grid. In both data sets dominant NOx emissions sources can easily be identified: (large) cities, shipping lanes, corridors between large cities consisting of roads and smaller cities and towns along these corridors. There is also a striking difference: DECSO emissions in rural and non-populated areas are much larger than in the TNO database. This is caused by soil emissions, which simply are not present in the TNO industrial 2010 NOx emission database.

TNO total NOx emissions for this region are 1.49/1.36 Tg/year for 2010 and 2015, respectively, while total DECSO NOx emissions for the same region amount to 2.55 Tg/year. If only pixels are considered where TNO NOx emissions are larger than 0.1 Tg, then DECSO NOx emissions are 1.41/1.37 Tg/year, respectively.

A difference plot of TNO and DECSO NOx emission (not shown) indicated that there appear to be some pixel-by-pixels shifts in emissions. This can be related to the information going into the bottom-up TNO emission database not being spatially very accurate at the grid scale. For example, emissions often are reported per city region or province. Based on other information, these emissions will then be redistributed to the smaller grid, but this inevitably will introduce spatial uncertainties and inaccuracies, even though the total emissions for the city region or province may be accurate.

To account for this, figure 4 shows a scatterplot of total NOx emissions per 2°×2° grid, but only considering the 1/8 grid points for which the TNO NOx emissions were larger than 0.1 Tg/gridpoint. The 2°×2° averaging should – to some extent – account for the spatial uncertainties and inaccuracies introduced by the high resolution redistribution process. Clearly, at this 2°×2° resolution there is an excellent agreement between the TNO and DECSO emissions. The high bias of approximately 20% of TNO compared to DECSO may be related to the years they represent (2010 vs. July 2018 – June 2019).
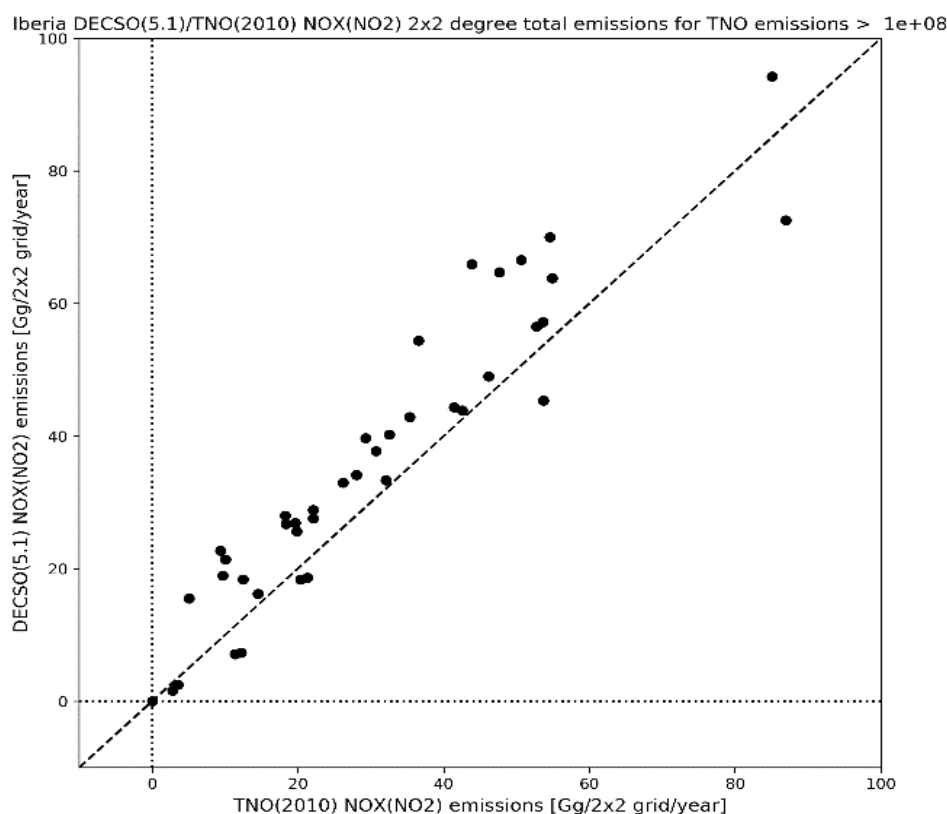

Figure 4. Scatterplot of Iberian TNO (2010) and DECSO (July 2018 – June 2019) total NOx emissions at a 2°x2° grid. To account for the biogenic NOx emission in DECSO that are not part of the TNO database, only 1/8° grid points with TNO emissions larger than 0.1 Gg are included in calculating the 2°x2° grid average.

3.5 Comparison to an Argentinian bottom-up inventory

We have compared the DECOS emission to an Argentinean bottom-up emission inventory recently published in Puliafito et al.(2020). The inventory contains emission for the year 2014 and 2016. We have resampled the 2016 NOx emissions to the same grid as of DECSO for comparison. Figure 5 shows the comparison between the annual bottom-up and the annual averaged NOx emissions of DECSO. The inventories disagree on two points:

1. The emissions from traffic in Puliafito are very prominent in the figure, with traffic emissions amounting to 50% of the total emissions. In the DECSO emissions the road-map of Argentina cannot be distinguished. When the traffic emissions are reduced by 75% in Puliafito, the emissions are comparable (see Figure 6).

2. Agricultural emissions are much higher in the DECSO map as can be seen in the Northern part of Argentina, where many agricultural communities exist.
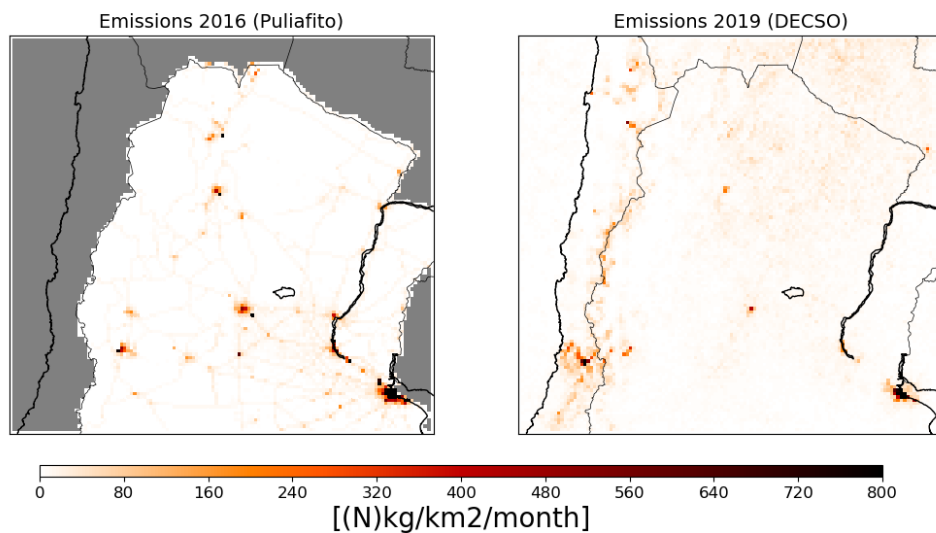
Figure 5 Comparison of the NOx emissions over Argentina from the bottom-up inventory in 2016 (left plot) and the DECSO emissions in 2019 (right plot).
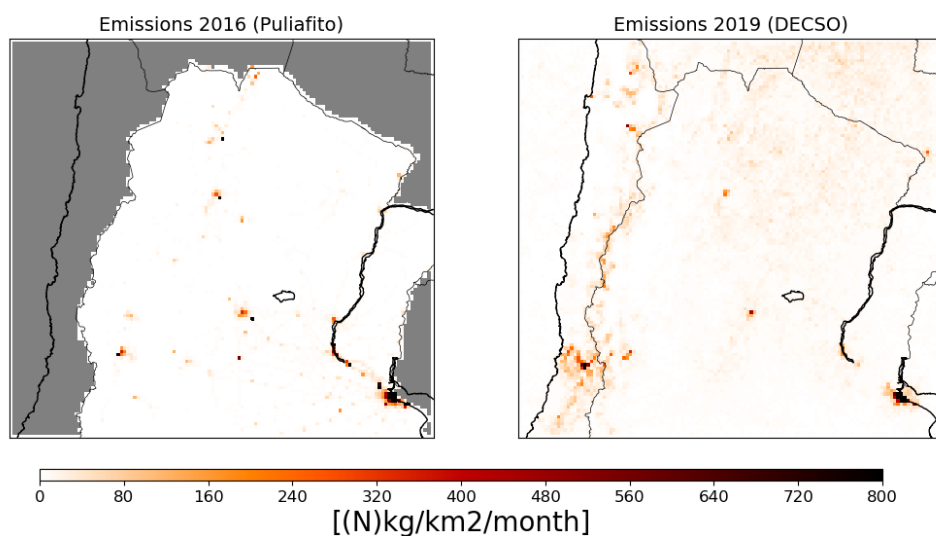
Figure 6 Same as Figure 5, but with traffic emissions reduced by 75% in the bottom-up inventory.

Reference:
S. E. Puliafito, T. Bolaño-Ortiz, L. Berná, R. P. Flores, High resolution inventory of atmospheric emissions from livestock production, agriculture, and biomass burning sectors of Argentina, Atm. Environment, 223, 117248, doi:10.1016/j.atmosenv.2019.117248, 2020.

4 Time series of DECSO emissions

Two examples of times series of typical emissions are given in the Figures below. The top figures shows the timelines of emissions in the Brazilian cities Sao Paulo, Rio de Janeiro, Porto Alegro, the Argentinean capital Buenos Aires and the Chilean capital Santiago. The cities have higher emissions in wintertime compared to summertime (Southern hemisphere).
In addition the emissions of the Lula oil field on the Atlantic Ocean south of Rio de Janeiro are shown. The Lula oil field is one of the largest on the Western hemisphere.
The lower plot shows the emissions of an agricultural area in Chaco in North Argentina. The seasonal cycle clearly shows a peak in February and almost no emissions in July when the temperature is low.
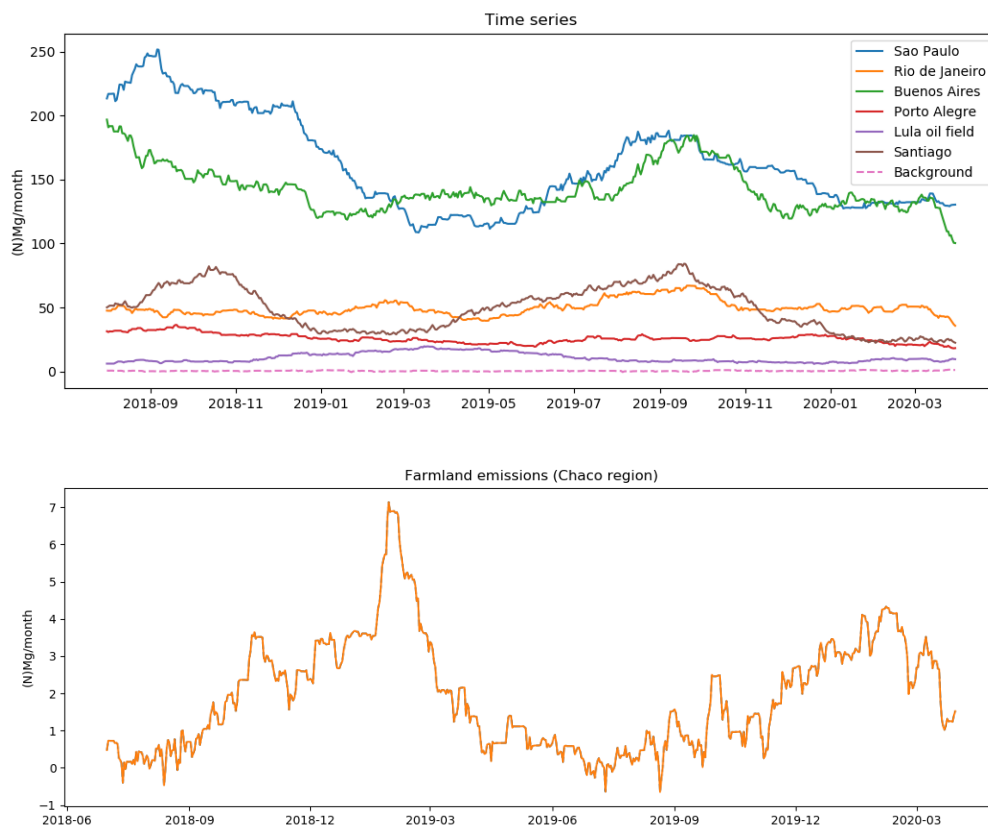
Figure 7 Timeseries of (a) emissions from cities in South America and (b) emissions from an agricultural region in Chaco, Argentina.

5 NOx emission publications

Ding, J., R.J. van der A, B. Mijling, P.F. Levelt and N. Hao, NOx emission estimates during the 2014 Youth Olympic Games in Nanjing, Atm. Chem. Phys., 2015, 15, 9399-9412, doi:10.5194/acp-15-9399-**2015**.

Ding, J., van der A, R. J., Mijling, B., Jalkanen, J.-P., Johansson, L. and Levelt, P. F., Maritime NOx emissions over Chinese seas derived from satellite observations. Geophysical Research Letters, 45. https://doi.org/10.1002/2017GL076788, **2018.**

Ding, J., Miyazaki, K., van der A, R.J., Mijling, B., Kurokawa, J., Cho, S., Janssens-Maenhout, G., Zhang, Q., Liu, F., and Levelt, P.F., Intercomparison of NOx emission inventories over East Asia, Atm. Chem. Phys., **2017**, 17, 10125-10141, doi:doi.org/10.5194/acp-17-10125-2017.

Ding, J., R.J. van der A, B. Mijling and P.F. Levelt, Space-based NOx emission estimates over remote regions improved in DECSO, Atmospheric Measurement Techniques, **2017**, 10, 925-938, doi:10.5194/amt-10-925-2017.

Mijling, B. and R.J. van der A, Using daily satellite observations to estimate emissions of short-lived air pollutants on a mesoscopic scale. J. Geophys. Res. 117, D17, doi:10.1029/2012JD017817, **2012**.

Mijling, B., R.J. van der A and Q. Zhang, Regional nitrogen oxides emission trends in East Asia observed from space. Atmos. Chem. Phys., 13, 12003-12012, doi:10.5194/acp-13-12003-2013, **2013**.

van der A, R. J., Mijling, B., Ding, J., Koukouli, M. E., Liu, F., Li, Q., Mao, H., and Theys, N., Cleaning up the air: Effectiveness of air quality policy for SO2 and NOx emissions in China, Atm. Chem. Phys., **2017**, 17, 1775-1789, doi:10.5194/acp-17-1775-2017.

van der A, R.J., de Laat, A.T.J., Ding, J., Eskes, H.J., Connecting the dots: NOx emissions along a West Siberian natural gas pipeline, npj Clim Atmos Sci 3, 16, https://doi.org/10.1038/s41612-020-0119-z, **2020**.